Neutron scattering investigation of a diluted blend of poly(ethylene oxide) in polyethersulfone

A.-C. Genix, A. Arbe, S. Arrese-Igor, J. Colmenero, D. Richter, B. Frick, and P. P. Deen

Citation: The Journal of Chemical Physics **128**, 184901 (2008); doi: 10.1063/1.2918497
View online: https://doi.org/10.1063/1.2918497
View Table of Contents: http://aip.scitation.org/toc/jcp/128/18
Published by the American Institute of Physics

Neutron scattering investigation of a diluted blend of poly(ethylene oxide) in polyethersulfone

A.-C. Genix,[1] A. Arbe,[2,a)] S. Arrese-Igor,[2] J. Colmenero,[2,3,4] D. Richter,[5] B. Frick,[6] and P. P. Deen[6]

[1]*Laboratoire des Colloïdes, Verres et Nanomatériaux, UMR 5587 CNRS, Université Montpellier II, 34095 Montpellier, France*
[2]*Centro de Física de Materiales (CSIC-UPV/EHU), Apartado 1072, 20080 San Sebastián, Spain*
[3]*Departamento de Física de Materiales UPV/EHU, Apartado 1072, 20080 San Sebastián, Spain*
[4]*Donostia International Physics Center, Apartado 1072, 20080 San Sebastián, Spain*
[5]*Institut für Festkörperforschung, Forschungszentrum Jülich GmbH, D-52425 Jülich, Germany*
[6]*Institut Laue-Langevin, BP 156, 38042 Grenoble Cedex 9, France*

(Received 6 December 2007; accepted 8 April 2008; published online 8 May 2008)

By using quasielastic neutron scattering (QENS) with isotopic labeling we have investigated the component dynamics in a miscible blend of polyethersulfone (PES) and poly(ethylene oxide) (PEO) with 75% content in weight of PES. Due to the large difference in the glass-transition temperatures, T_g's, of the two polymers ($T_g^{\mathrm{PEO}} \approx 220$ K, $T_g^{\mathrm{PES}} \approx 382$ K) the dynamic asymmetry in the system dramatically increases when approaching the average T_g of the blend, $\langle T_g^{\mathrm{blend}} \rangle$. For the fast (PEO) component, this leads to a behavior which hints a crossover from typical glass-forming liquidlike dynamics at high temperatures to confined dynamics close to $\langle T_g^{\mathrm{blend}} \rangle$ induced by the freezing of the segmental motions of the slow PES. The features of the confined PEO motion observed by QENS are similar to those of the secondary γ-relaxation detected for pure (semicrystalline) PEO. A neutron diffraction study of the short-range order of the homopolymers and the blend suggests that this coincidence could be due to similarities in the intermolecular packing of PEO and PES polymers. © *2008 American Institute of Physics*. [DOI: 10.1063/1.2918497]

I. INTRODUCTION

Blends based on thermodynamically miscible polymers are to date one of the most efficient and economical means to produce new materials with tailored properties. Thus, the dynamical behavior of each component in binary polymer blends has attracted increasing interest and the question of the dynamic miscibility, i.e., how exactly the molecular motions of each component in a miscible blend are modified by blending, has come into focus (see, for instance, Refs. 1–10). By now, dynamic heterogeneity is a well established feature of polymer blends, which refers to the observation of two different characteristic timescales for segmental relaxation, each of them corresponding to the dynamics of each component modified by blending. A large experimental effort has been devoted to the phenomenological characterization of this effect and, nowadays, it is commonly accepted to be mainly a consequence of the enhancement of the local concentration around a given segment on its own component due to chain connectivity (the so-called self-concentration effect).[1,11]

The dynamic heterogeneity induces a dynamic asymmetry in the blend system which is magnified under extreme conditions. At atmospheric pressure, three ingredients allow tuning this asymmetry: (i) the blend composition (dilution of one of the components), (ii) the difference in the dynamics of the pure polymers (larger differences in the original glass-transition temperatures, T_g's, lead to more distinct timescales for segmental relaxations), and (iii) the temperature (due to the non-Arrhenius-type temperature dependence of the α-relaxation, the dramatic increase of the timescale of each component approaching its own glass transition leads to the enhancement of the asymmetry when cooling down). Thus, playing with these ingredients a huge dynamic asymmetry may be induced in the system, leading to the possible emergence of confinement-like effects on the dynamics of the minority low-T_g component when approaching the average glass transition of the blend, $\langle T_g^{\mathrm{blend}} \rangle$. First experimental evidence of this behavior was reported from dielectric spectroscopy (DS) studies for poly (vinyl methyl ether) (PVME) ($T_g^{\mathrm{PVME}} = 249$ K) blends with high concentrations of polystyrene (PS) ($T_g^{\mathrm{PS}} = 373$ K).[12] Although in those conditions a confinement length cannot be easily defined, a value of about 10 Å (i.e., double the intermolecular distance) was suggested for extreme dilution of PVME in PS. However, dielectric spectroscopy does not provide the spatial information necessary to fully characterize the dynamics of the fast component.

The required space/time resolution at molecular level is offered by neutron scattering techniques, which allow, in addition, the selective study of one of the blend components by deuteration of the other polymer chains. This strategy has been repeatedly used to investigate the segmental relaxation of blend components in miscible blends of compositions close to 50%/50%.[13–17] However, in these systems, the possible confinement effects induced by the differences in glass-

a)Electronic mail: waparmea@sc.ehu.es.

transition temperatures of the homopolymers would be expected to be less evident, mainly in the high temperature range accessible by QENS.

The first direct microscopic observation of the confinedlike blend dynamics by neutron scattering was realized on poly(ethylene oxide) (PEO) in blend with poly(methyl methacrylate) (PMMA) with a low concentration of PEO.[18] The T_g's of these homopolymers differ by almost 200 K. This system was studied by quasielastic neutron scattering (QENS) using the backscattering technique in a sample where the high-T_g majority component (PMMA) was fully deuterated. In this way, the scattering intensity is mainly dominated by the incoherent scattering from PEO hydrogens which allows tracking of the self-motion of this fast component. In the whole temperature region explored by the QENS study on PEO/PMMA, confinementlike effects were noticed for the PEO component.[18] These effects were deduced from the extremely stretched functional forms shown by the scattering functions. In fact, broad distributions of relaxation times with T-dependent width had to be invoked in order to describe the experimental results. Moreover, deviations of the timescales with respect to the expected behavior in regular blends (e.g., provided by the Lodge and McLeish model[1] based on self-concentration ideas) were found. The combination with fully atomistic molecular dynamics (MD) simulations suggested the occurrence of localized and heterogeneous motions of PEO within the frozen PMMA matrix in this regime.[18] Extremely broad distributions of relaxation times were also reported for PEO in blends with PMMA at different concentrations (10%–30% PEO) from a QENS investigation of García Sakai *et al.*[19] There, the concept of local composition was emphasized as a key ingredient for the PEO dynamics. In those experiments, the PEO dynamics was selectively studied using partially protonated blends in a similar way as in Ref. 18. In another work of the same group,[20] the collective dynamics of fully deuterated blends (dPEO/dPMMA) was addressed by means of neutron spin echo. The analysis of the structure factor decays with a single stretched exponential delivered very small stretching parameters. Deviations of the such obtained characteristic times towards the β-relaxation of pure PMMA were also reported in the neighborhood of $\langle T_g^{\text{blend}} \rangle$. We note that those experiments are not selective for the PEO component in the blend and the interpretation of the results is thus extremely complicated without the help of, e.g., MD simulation to disentangle the different contributions to the structure factor.

Confinement effects on PEO dynamics upon blending were also found in a selective QENS investigation of the system hPEO/d-poly(vinyl acetate) (PVAc) (20%/80%), where the difference between the homopolymers T_g's is about 100 K.[21] In that work, the results showed the existence of a crossover temperature located at $\approx$70 K above the calorimetric $\langle T_g^{\text{blend}} \rangle$, for the dynamics of PEO in the blend: at high temperatures, the PEO behavior is rather close to that expected for a "standard" glass-forming system in supercooled regime, whereas signatures of confined dynamics were observed when decreasing the temperature toward $\langle T_g^{\text{blend}} \rangle$.

The effect of blending on the majority high-T_g component was also investigated in blends of PMMA/PEO,[18,22,23] and PVAc/PEO.[24] Maranas and coworkers[22,23] found that the dynamics of PMMA in hPMMA/dPEO blends was simply controlled by the distance above the glass transition of the blend. The PVAc component in hPVAc/dPEO showed a perfectly regular behavior in the framework of the self-concentration model.[24] It means that the dynamics of the majority high-T_g component does not seem to show any significant deviations from the standard behavior observed in regular blends. We mention also the study on 1,4-cis-polyisoprene (PI) in blend with 1,2-polybutadiene (PVE) with a composition of 70% PI–30% PVE (i.e., highly asymetric in composition), where the dynamics of both components were selectively addressed by QENS.[17] It is noteworthy that, in this case, the majority component (PI) is that of the lowest T_g (i.e., more mobile). Interestingly, in this blend, the segmental relaxation of the minority component (PVE) was found to resemble that of PI.

The confinementlike features for the low-T_g component are a consequence of the nonequilibrium situation reached in the vicinity of $\langle T_g^{\text{blend}} \rangle$. There, the chain and segmental dynamics of the matrix could be considered as completely frozen on the time scale of the segmental motions of the fast low-T_g component. In that situation, localized and rather heterogeneous motions of the fast component are expected. In fact, a recent study on PEO/PMMA blends addressing the single chain dynamics of PEO (extending thereby the range of observation towards larger length scales) strongly suggests the existence of a broad distribution of monomeric friction coefficients.[25] In that work, it is shown that such a distribution can be deduced from the heterogeneous segmental (short-scale) motions of PEO in the blend. On the other hand, it has been found that the short-scale dynamics of PEO in PMMA and PVAc show very similar features in the low-temperature region close to $\langle T_g^{\text{blend}} \rangle$ (for the time scale and also for the width of the relaxation time distributions).[21] Thus, the question arises: is the localized process reported for PEO completely independent of the nature of the surrounding polymer? In this case, the localized motions would be universal for PEO and the location of the crossover from "standard" to confined dynamics would depend exclusively on the relaxation time of the high-T_g component's segmental motions. However, other ingredients related, e.g., with the structure at interchain level and/or specific interactions between the two components may also play a role in this game.

With these ideas in mind, we have investigated the dynamics of the PEO component diluted in another blend, namely, with polyethersulfone (PES), which is a well-known engineering thermoplastic. Again exploiting the advantages of QENS combined with isotopic labeling, we have studied with a backscattering spectrometer a blend of protonated PEO with deuterated PES (dPES). In this way, we could access the PEO dynamics at time scales in the nanosecond range and length scales of the order of typical interchain distances. Though the deuterated dPES used was a rather low-molecular weight polymer, the difference in T_g's of the two homopolymers is still very high, about 160 K. The QENS measurements were performed in a wide temperature range—above and below $\langle T_g^{\text{blend}} \rangle$—where it was possible to

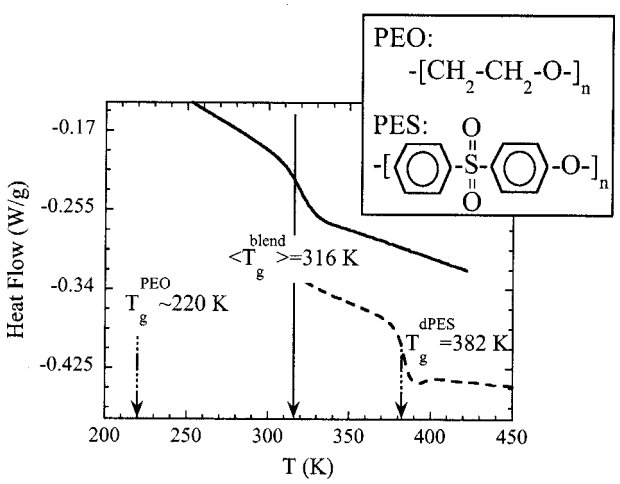

FIG. 1. DSC traces for the PEO/dPES blend sample (solid line) and for the pure dPES sample (dashed line). The cooling rate was 10 K/min. The insert shows the chemical structures of PEO and PES.

observe two distinct behaviours of the self-motion of PEO. In addition to the investigation of the dynamics, we have addressed a structural study on both, dPES and the blend by using neutron diffraction. Thereby, the short-range order of the two systems has been scrutinized. In the case of the blend, this study has been realized by using polarization analysis, which has allowed the separation of coherent and incoherent contributions to the total scattered intensity. Such information is also very important to assure a proper analysis of the QENS data. On the other hand, the comparison of the structural properties revealed by the structure factors of the polymers involved in the various blends considered in our discussion, PES, PMMA,[18] PVAc,[21] and PEO,[26] can help to understand the origin of our results.

II. EXPERIMENT

A. Samples

The samples investigated in this study are fully deuterated polyethersulfone (dPES) and a blend of protonated poly (ethylene oxide) (PEO) and dPES consisting of 25% PEO in weight. The deuteration level of dPES was about 93%, as deduced from proton NMR in DMSO-d6 (CD_3SOCD_3). For the preparation of the blend, dried PEO and dPES were dissolved in deuterated dimethylformamide (DMF) in appropriate quantities to obtain a 5% solution that has been slowly casted in a dessicator under vacuum at 333 K. The miscibility in PEO/PES mixtures obtained under such conditions was investigated by Guo and Higgins.[27] It was found that PEO and PES are miscible in a wide range of temperature and composition. Moreover, there was no hint of PEO crystallization for PEO content $\leqslant 50\%$ in the blend at room temperature.[27] The molecular weights M_w of the polymers involved are $M_w(\text{dPES})=9$ kg/mol and $M_w(\text{PEO})=43$ kg/mol. The polydispersities (M_w/M_n) are 1.05 and 1.5 for PEO and dPES, respectively. The glass-transition temperature T_g of both samples was determined by differential scanning calorimetry (DSC) measurements considering the middle points of the DSC scans at 10 K/min, as shown in Fig. 1. We found $T_g^{\text{dPES}}=382$ K and $\langle T_g^{\text{PEO/dPES}}\rangle=316$ K, being in the last case the step in the heat capacity much more extended in temperature as is typical for polymer blends. Each sample was vaccuum heated near T_g for at least 24 h prior to the measurements, in order to remove any moisture content.

B. Neutron scattering measurements

Information on the structure and dynamics of a sample can be obtained by analyzing the change in energy ($E=\hbar\omega$) experienced by neutrons scattered into a given solid angle between Ω and $\Omega+d\Omega$.[28–31] The modulus of the momentum transfer Q ($\mathbf{Q}=\mathbf{k}_f-\mathbf{k}_i$) is determined by the scattering angle θ and the wavelength of the incoming neutrons λ as $Q=4\pi\sin(\theta/2)/\lambda$. The measured double differential scattering cross section $\partial^2\sigma/\partial\Omega\partial E$ contains incoherent and coherent contributions.

The incoherent cross section $(\partial^2\sigma/\partial\Omega\partial E)_{\text{inc}}$ is given by the product of the incoherent scattering cross section σ_{inc} and the incoherent scattering function $S_{\text{inc}}(Q,\omega)$, $(\partial^2\sigma/\partial\Omega\partial E)_{\text{inc}}=N(k_f/k_i)\sigma_{\text{inc}}S_{\text{inc}}(Q,\omega)/(4\pi)$. N is the number of nuclei in the sample. $S_{\text{inc}}(Q,\omega)$ is related via Fourier transformation with the intermediate incoherent scattering function, $S_s(Q,t)$. Its double Fourier transform is the self-part of the Van Hove correlation function, $G_s(r,t)$. In the classical limit, $G_s(r,t)$ is the probability of a given nucleus to be at a distance r from the position where it was located at a time t before. Thus, incoherent scattering looks at correlations between the positions of the same nucleus at different times.

The coherent scattering deals with relative positions of atomic pairs, i.e., the collective features. Its double differential cross section can be expressed as

$$\left(\frac{\partial^2\sigma}{\partial\Omega\partial E}\right)_{\text{coh}}=N\frac{k_f}{k_i}\frac{\sigma_{\text{coh}}}{4\pi}S_{\text{coh}}(Q,\omega), \tag{1}$$

where $S_{\text{coh}}(Q,\omega)$ can be written as $S_{\text{coh}}(Q,\omega)=S(Q)\tilde{S}_{\text{coh}}(Q,\omega)$. The coherent differential scattering cross section $(\partial\sigma/\partial\Omega)_{\text{coh}}$ accessible in a diffraction experiment (isolated by polarization anlysis) reveals structural properties,

$$\left(\frac{\partial\sigma}{\partial\Omega}\right)_{\text{coh}}=\frac{\sigma_{\text{coh}}}{4\pi}S(Q)=\frac{1}{N}\left\langle\sum_{i,j=1}^{N}\bar{b}_i\bar{b}_j e^{i\mathbf{Q}\mathbf{r}_{ij}}\right\rangle. \tag{2}$$

Here, the $\bar{b}_i$ stand for the coherent scattering lengths for neutrons (see Table I). $\mathbf{r}_{ij}=\mathbf{r}_i-\mathbf{r}_j$ is the vector connecting atoms i and j at the same time, and the brackets denote the thermal average. The $Q\to\infty$ limit of the coherent differential cross section is determined by the coherent cross section σ_{coh},

$$\lim_{Q\to\infty}\left(\frac{\partial\sigma}{\partial\Omega}\right)_{\text{coh}}=\frac{1}{N}\sum_{i=1}^{N}\bar{b}_i^2=\frac{\sigma_{\text{coh}}}{4\pi}. \tag{3}$$

The other function in Eq. (1), $\tilde{S}_{\text{coh}}(Q,\omega)$, is the normalized coherent cross section (area=1) carrying the dynamical information. Correspondingly, the Fourier transform $\tilde{S}_{\text{coh}}(Q,t)$ takes the value 1 for time equals 0.

In a sample with different kinds of isotopes their contributions to the scattered intensity are weighted by the corre-

TABLE I. Scattering length (fm) and coherent and incoherent cross sections (barns) of the isotopes involved. The cross sections are also given for the samples investigated (in units of barn/monomer) assuming 100% deuteration for dPES.

Nucleus/sample	$\bar{b}$	σ_{coh}	σ_{inc}
H	−3.7406	1.7583	80.26
D	6.671	5.592	2.05
C	6.6460	5.559	0
O	5.803	4.232	0
S	2.847	0.9880	0
hPEO/dPES			
$[(C_2H_4O)_1(C_{12}D_8O_3S)_{0.55}]_n$		91.204	330.072
dPES			
$[C_{12}D_8O_3S]_n$		125.128	16.419

sponding incoherent cross sections and scattering lengths. Table I shows the values of these functions for the different nuclei involved in our samples. It can be realized that the incoherent scattering cross section of hydrogen is much higher than the rest of the cross sections in the samples. Therefore, the intensity scattered by the blend PEO/dPES is clearly dominated by incoherent contribution of PEO protons ($\sigma_{inc}^{H(PEO)}/\sigma_{tot}^{PEO/dPES}=0.72$, taking into account the 93% deuteration of dPES). Thus, quasielastic experiments on this sample provide information on PEO dynamics in the blend by following its hydrogen motions. However, as dPES is the majority component in the blend, there is a non-negligible (mainly coherent) contribution of dPES to the scattered intensity. On the other hand, the scattering of the pure deuterated sample dPES is predominantly coherent and, as the cross sections of the constituting nuclei are very similar, the differential cross section measured in a diffraction experiment directly delivers the structure factor of this homopolymer.

1. Structural studies (diffraction): D7 and D20

To determine the coherent and incoherent scattering cross sections of the blend sample, we used polarization analysis at the diffuse scattering spectrometer D7 at the Institut Laue-Langevin (ILL), in its diffraction mode. Incoherent scattering arising solely from spin disorder flips the neutron spin with probability of 2/3, while coherent scattering leaves the spin unchanged. Therefore, using polarized neutrons, it is possible to separate both kinds of contributions to the scattered intensity. For the measurements, the incident wavelength was set to 4.8 Å enabling a range of scattering vectors Q up to 1.95 Å^{-1}. The experiments were performed at 130, 250, 300, 350, 400, and 450 K.

The structural characterization of dPES was realized on the two-axis diffractometer D20 located at the ILL and characterized by a very high neutron flux. Using an incident wavelength of 1.3 Å the total differential cross section (highly dominated by the coherent contribution, see Table I) was investigated in the Q range of 0.6–9.3 Å^{-1}. A cylindrical vanadium sample holder was used to avoid Bragg peaks from the container. The measurements were performed between 100 and 400 K every 50 K with measuring times of 20 min at each temperature, providing excellent statistics. In both diffraction experiments, the contribution from the sample holder was measured and properly subtracted from the original data.

2. Dynamics study (quasielastic): IN10

The QENS measurements on the blend PEO/dPES were carried out by means of the IN10 backscattering spectrometer at the ILL. The incident energy is changed by applying a Doppler shift using a moving monochromator crystal. Using $\lambda=6.271$ Å, the energy window of the experiment was set to $-12.3\ \mu\text{eV}\leqslant\hbar\omega\leqslant 12.3\ \mu\text{eV}$, accessing seven different Q values in the range between 0.50 and 1.96 Å^{-1}. The energy resolution was about 1.1 μeV [full width at half maximum (FWHM)]. The sample, directly casted inside a flat aluminium container, had a thickness of 0.5 mm providing a transmission of 90%. It was positioned at 45° with respect to the incident beam. We investigated temperatures from 250 to 400 K every 25 and 420 K, with measuring times of the order of 20 h at each temperature. As NS spectrometers offer a limited energy resolution, the measured functions are affected by the instrumental resolution function $R(Q,\omega)$. Thus, the experimentally accessed quantity has to be compared with the convolution of the model function and the resolution, $I_{exp}\sim I(Q,\omega)\otimes R(Q,\omega)$. $R(Q,\omega)$ is the obtained spectrum when purely elastic ($\hbar\omega=0$) scattering events take place in the sample [i.e., it is the "image" of $\delta(\omega)$]. In this case it was determined from a measurement of the sample at 5 K. Background corrections were performed by subtracting the scattering from the empty cell. The detector efficiency was corrected by a vanadium measurement. For the data correction, we used the standard program SQW available at the ILL.

III. RESULTS AND DATA ANALYSIS

A. Structure

Figure 2(a) shows the temperature dependence of the ratio between the coherent and incoherent differential cross sections measured by D7 on the blend. These data are of utmost importance for the analysis of our quasielastic results. They show that, as expected (Table I), in the Q range covered by IN10 ($0.5\ \text{Å}^{-1}\leqslant Q\leqslant 2\ \text{Å}^{-1}$) the incoherent signal is in average about three times stronger than the coherent one for all temperatures investigated. In addition, we can extract valuable structural information from these results, provided by the Q dependence of the coherent signal.[32] Its dramatic increase in the low-Q region is due to the contrast between deuterated and protonated chains, and contains information on the dimensions of the chains and the interaction between them (see, e.g., Refs. 33 and 34). On the other hand, in the Q range above ≈ 0.5 Å^{-1}, the oscillations of the measured intensities reflect the short-range order present in the sample. As the coherent scattering arises mainly from the deuterated dPES component constituting the 75% in weight of the sample, it basically mirrors there the structure factor $S(Q)$ of this component in the blend ($\sigma_{coh}^{dPES}/\sigma_{coh}^{blend}=0.755$). The main feature observed is a broad peak centered at about 1.5 Å^{-1}, which does not appreciably depend on temperature below 300 K (i.e., in the glassy state of the blend). A slight shift of

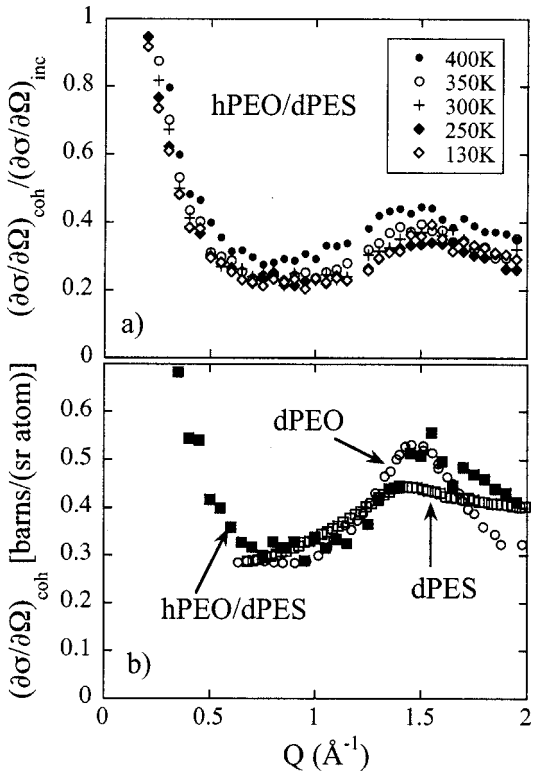

FIG. 2. (a) Ratio between the coherent and the incoherent intensities obtained from D7 measurements for the blend PEO/dPES at different temperatures: 130 K (empty diamonds), 250 K (full diamonds), 300 K (pluses), 350 K (empty circles), and 400 K (full circles). In (b) the coherent cross section obtained for the blend at 130 K (full squares) is compared with those estimated for the fully deuterated homopolymers: dPES at 150 K (empty squares) and dPEO (empty circles) (Ref. 26). For the calculation of the absolute units in the blend and dPES, the 93% deuteration level of dPES has been considered. This has also been assumed for subtracting the incoherent level of the dPES D20 data. In the case of dPEO, the data have been multiplied by an appropriate factor to get approximately the theoretical limit at high Q.

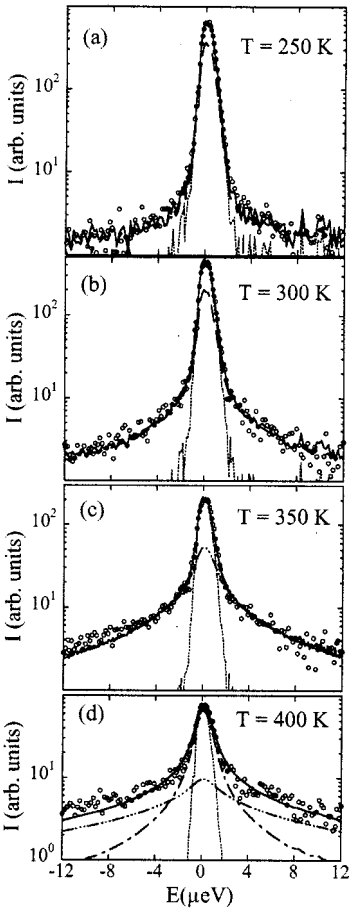

FIG. 3. Neutron scattering spectra obtained by IN10 on the PEO/dPES sample at $Q=1.45$ Å^{-1} and several temperatures: 250 K (a), 300 K (b), 350 K (c), and 400 K (d). The dashed-dotted lines show the contribution of the fast component (PEO) modeled through a log-normal distribution of relaxation times. The solid lines show the sum of such quasielastic component and the coherent contribution, which in (a), (b), and (c) is just elastic, while in (d) it shows a broadening depicted by the dashed line (Fourier transform of a KWW function with $\beta=0.5$). The dotted lines show the instrumental resolution obtained at 5 K (normalized to match the data in the maximum).

the peak position toward lower Q values can be envisaged at 350 K and a clear increase in intensity is observed at 400 K.[32] Such behavior suggests a predominantly intermolecular nature of this main peak, since only the interchain correlations are expected to appreciably evolve above the glass-transition temperature of the system (see, e.g., Ref. 35).

The comparison of the blend data with the structure factor of the pure homopolymer dPES measured on D20 is done in Fig. 2(b). The main peak of $S(Q)$ in dPES is located at $Q\approx 1.44$ Å^{-1}. This value is rather close to that where the blend shows the main peak, suggesting that the short-range order in this polymer is hardly affected by the presence of PEO chains—at least for the concentration here investigated. A further comparison with the structure factor of PEO measured on the deuterated sample dPEO (Ref. 26) [Fig. 2(b)] reveals that the intermolecular packing is rather similar also in both homopolymers. After such observation, it appears logical that the main interchain distances remain the same when the two polymers are blended.

B. Dynamics

As can be appreciated in Fig. 3 for a representative Q value, the IN10 spectra are broadened with respect to the instrumental resolution even at temperatures well below the calorimetric glass transition of the blend ($\langle T_g^{PEO/dPES}\rangle = 316$ K). This broadening can also be appreciated in a linear representation of the data directly compared with the resolution, as shown in Fig. 4. The quasielastic intensity—indicative for a decay of the intermediate scattering function at timescales in the nanosecond range—increases with increasing temperature. For an intermediate temperature, Fig. 5 shows how the spectra evolve with momentum transfer.

As expected from the values of the cross sections of the blend components (Table I) and experimentally proven by the D7 measurements [Fig. 2(a)], the IN10 spectra mainly reveal the incoherent scattering from PEO hydrogens (the rest of the incoherent scattering, due to dPES deuterons, can be neglected compared to it). However, Fig. 2(a) shows that a non-negligible part of the neutrons are scattered coherently (reflecting mainly dPES correlations) and this has to be also considered to properly describe the full IN10 curves. We may decompose our spectra into two main contributions,

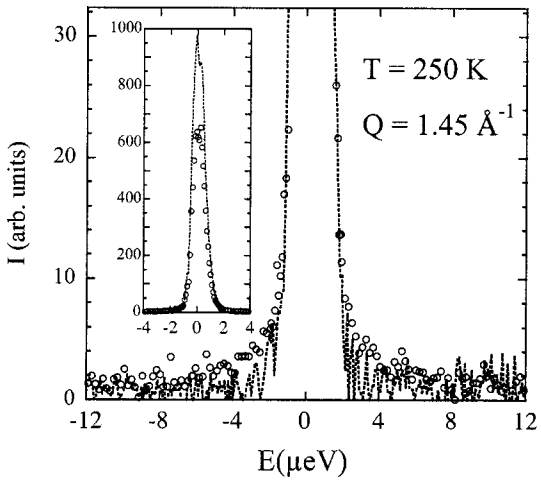

FIG. 4. The same data as shown in Fig. 3(a) are plotted in linear scale. In this case, the relative intensities between the data at 250 K and the resolution have not been modified for comparison. The maximum of the scale is 5% of the elastic intensity of the 250 K data (see full scale in the insert).

$$I(Q,\omega) = f_{\mathrm{PEO}}(Q) S_{\mathrm{inc}}^{\mathrm{H,PEO/blend}}(Q,\omega) + f_{\mathrm{coh}}(Q) \tilde{S}_{\mathrm{coh}}(Q,\omega). \tag{4}$$

The first—and dominant—one is attributed to the incoherent contribution from the PEO hydrogens and its weight, $f_{\mathrm{PEO}}(Q)$, can be approximated by the incoherent cross section determined from the D7 study. The second one corresponds to the contribution associated with the coherent scattering and weighted by $f_{\mathrm{coh}}(Q)$, that is obtainable from the coherent cross section measured by D7. The scattering functions $S_{\mathrm{inc}}^{\mathrm{H,PEO/blend}}(Q,\omega)$ and $\tilde{S}_{\mathrm{coh}}(Q,\omega)$ are normalized (total area =unity), and their parametrization requires the choice of a functional form.

Following the analysis previously applied to the QENS results on PEO in other blends [with PMMA (Ref. 18) and with PVAc (Ref. 21)] we have assumed that the coherent contribution is elastic close and below $\langle T_g^{\mathrm{blend}} \rangle$, where the structural relaxation of PES should be either too slow to be detected by QENS or even frozen. The correctness and possible consequences of this approximation will be discussed later. However, at high temperatures, the coherent contributions from the segmental PES dynamics might be fast enough to contribute to the quasielastic scattering in the IN10 window. It is well known that the relaxation function of the α-relaxation (slow decay of the correlations) in a glass-forming liquid is usually described by stretched exponential or Kohlrausch–Williams–Watts (KWW) functions. Equivalently, this functional form has been found to be adequate to account for the intermediate scattering function associated with this relaxation,[36] and its Fourier transform describes the scattering function in the frequency domain,

$$S^{\mathrm{KWW}}(Q,\omega) = FT\left\{ \exp\left[-\left(\frac{t}{\tau_w(Q,T)} \right)^{\beta} \right] \right\}. \tag{5}$$

Here, the characteristic time τ_w may depend on both T and Q. In the relatively high-temperature range above the glass transition usually explored by NS, the β values are found between 0.4 and 0.6 for most of the polymers investigated.[36]

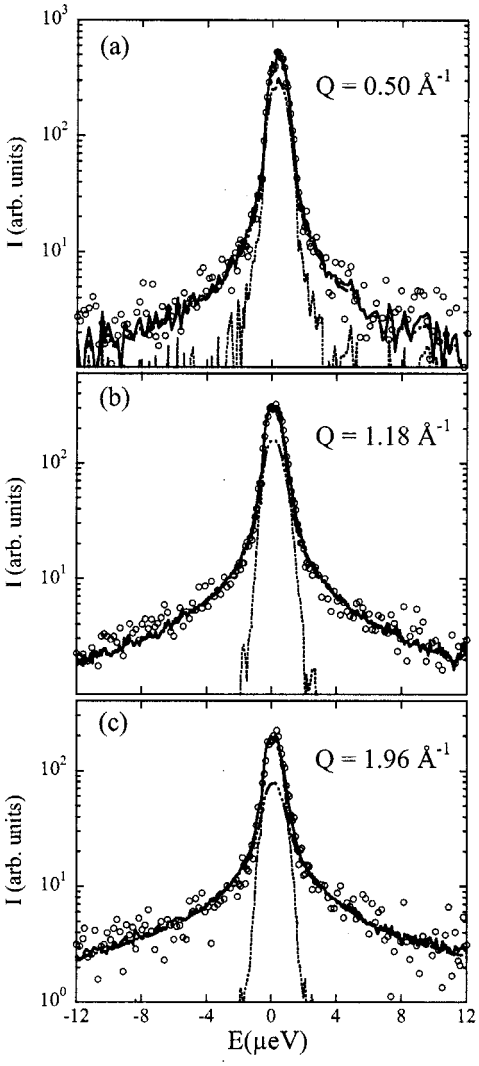

FIG. 5. IN10 spectra obtained for PEO/dPES at 325 K and different Q values: 0.50 Å^{-1} (a), 1.18 Å^{-1} (b), and 1.96 Å^{-1} (c). Lines like in Fig. 4.

Therefore, a typical value of β=0.5 has been assumed for the coherent contribution $\tilde{S}_{\mathrm{coh}}(Q,\omega)$ above $\langle T_g^{\mathrm{blend}} \rangle$.

In the case of the low-T_g component (PEO) we expect a different scenario when approaching $\langle T_g^{\mathrm{PEO/dPES}} \rangle$. There, this component is in a situation clearly different from that of the supercooled liquid state: PEO segments are surrounded by a more or less rigid polymer that is frozen as compared to the PEO characteristic time scale for structural relaxation. Therefore, it is expected that dPES imposes strong geometrical constraints (confinementlike) on the rapid PEO segmental motions. In confinement the structural relaxation is often observed to be modified[37] and behaving similar to more local relaxations such as, for instance, the secondary (Johari–Goldstein β) relaxation[38,39] or the methyl-group rotations.[40] The relaxation function (or scattering curve) of this type of processes is usually well described by broad and symmetric distribution functions of relaxation times directly connected with Gaussian-type distributions of activation barriers (heterogeneous behavior). Therefore, we can expect that also in the present conditions the PEO slow dynamics is no longer described by a KWW function and a log-normal distribution $g(\log \tau)$ of relaxation times seems to be a more appropriate

phenomenological function for $S_{\mathrm{inc}}^{\mathrm{H,PEO/blend}}(Q,\omega)$.[12,18,21] In the frequency domain, the scattering function is built by the superposition of Lorentzian functions appropriately weighted by $g(\log\tau)$

$$S^{g}(Q,\omega)=\int_{-\infty}^{+\infty} g(\log\tau)\frac{1}{\pi}\frac{\tau}{1+\omega^{2}\tau^{2}}d(\log\tau), \tag{6}$$

where the distribution is characterized by the width σ and the position of its maximum $\log\tau_o$,

$$g(\log\tau)=\frac{1}{\sqrt{2\pi}\sigma}\exp\left[-\frac{(\log\tau-\log\tau_o)^2}{2\sigma^2}\right]. \tag{7}$$

Finally, we have to take into account that the functions assumed in Eqs. (5) and (6) describe the *slow* decay of the intermediate scattering function which takes place after some picoseconds. In fact, in order to reproduce well the total intensity of the spectra, we have to consider the decay of the correlation functions produced by the *fast* dynamical processes (vibrations, Boson peak,…[36,41]) in the microscopic regime below ≈2 ps. In the dynamic window accessed by IN10, this can be parametrized in terms of a Debye–Waller factor (DWF),[42]

$$\mathrm{DWF}=\exp\left(-\tfrac{1}{3}\langle u^{2}\rangle Q^{2}\right), \tag{8}$$

which affects the amplitudes of the functions in Eqs. (5) and (6) when building the normalized $S_{\mathrm{inc}}^{\mathrm{H,PEO/blend}}(Q,\omega)$ and $\tilde{S}_{\mathrm{coh}}(Q,\omega)$,

$$S_{\mathrm{inc}}^{\mathrm{H,PEO/blend}}(Q,\omega)=\mathrm{DWF}_{\mathrm{PEO}}S^{g}(Q,\omega), \tag{9}$$

$$\tilde{S}_{\mathrm{coh}}(Q,\omega)=\mathrm{DWF}_{\mathrm{PES}}S^{\mathrm{KWW}}(Q,\omega). \tag{10}$$

In principle, the values of $\mathrm{DWF}_{\mathrm{PEO}}$ and $\mathrm{DWF}_{\mathrm{PES}}$ could be different. However, the values usually found for the effective vibrational mean-squared displacement, $\langle u^2\rangle$, in polymers can be considered rather similar within some limits (see, e.g., Ref. 13). Therefore, in order to reduce the number of fitting parameters in our analysis, we have assumed the same amplitudes for both scattering functions.

Taking into account all the above considerations for the terms involved in Eq. (4), the experimental IN10 data were fitted with the convolution of this expression with the resolution function. As can be seen in Figs. 3 and 5, the description of the scattering curves obtained by this procedure is very good.

IV. DISCUSSION

The analysis of the QENS spectra showed that the coherent contribution attributable mainly to dPES can be successfully described by an elastic peak for temperatures of the order of 350 K and below. Contrarily, at 375 K and above, the spectra cannot be longer described assuming an elastic contribution with the relative weight determined from the diffraction data. Thus, we have to allow the coherent contribution to be quasielastic in this high-temperature range. As can be seen, e.g., in Fig. 3(d), this contribution can be well accounted for by assuming Eq. (5) with β=0.5. The corresponding NS relaxation times decrease with increasing temperature, as can be seen in Fig. 6 for a Q value of 1.45 Å^{-1}. We note that this Q value is close to the partial structure factor peak Q_{max} revealing mainly dPES interchain correlations in this system, and therefore these spectra are sensitive to the dPES structural relaxation. Figure 6 shows also the characteristic relaxation times for the dielectric α-relaxation of dPES in the blend measured by standard dielectric relaxation techniques. The line through the points is a typical Vogel–Fulcher (VF) description,[43]

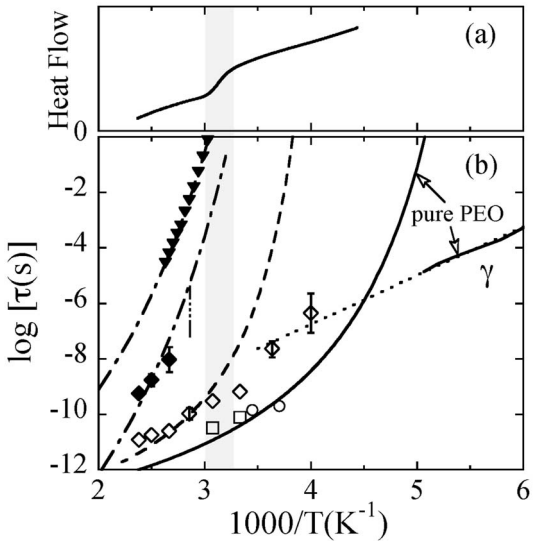

FIG. 6. (a) Calorimetric results for the blend PEO/PES. The shadowed area indicates the broad glass-transition region. (b) Temperature dependence of the characteristic times obtained for the two blend components in PEO/dPES by QENS at Q=1.45 Å^{-1} (empty diamonds: PEO; full diamonds: dPES). The DS time scales (inverse of the maximum frequency) of dPES in the blend are displayed for comparison as full inverted triangles. The dashed-dotted line through these points is a VF fit. The same VF has been shifted to match the QENS dPES data. The ends of the vertical dashed-dotted line indicate the two limiting approaches considered for the coherent contribution at 350 K. They lead to the error bar shown in the corresponding PEO time scale. The solid lines show the relaxation times of pure PEO [curved: segmental time, Arrhenius: γ process by DS (Ref. 51)]. The γ process is extrapolated towards high temperatures by the dotted line. The dashed line corresponds to the expectation for the PEO dynamics in the blend with dPES from the Lodge and McLeish model. Squares and circles show the timescales observed by QENS for PEO in blends with PMMA and PVAc, respectively.

$$\tau(T)=\tau_o\exp\left(\frac{B}{T-T_o}\right). \tag{11}$$

We observe that dPES dipoles relax with a longer characteristic time than that obtained by QENS close to Q_{max}. *A priori*, it cannot be predicted whether the time scales observed by different techniques (different projections of the α-relaxation) are faster or slower with respect to each other. For example, in the case of polybutadiene, dielectric spectroscopy and neutron spin echo on a fully deuterated sample at Q_{max} deliver similar time scales,[44] while for polyisoprene, the structural relaxation time scale at Q_{max} is slower than that observed for the dipole-dipole correlation function.[45] What it is believed is that the temperature dependence of the different projections of the structural relaxation should be the same (see, e.g., Ref. 46). In this direction, we observe that the temperature dependence of the QENS data is compatible

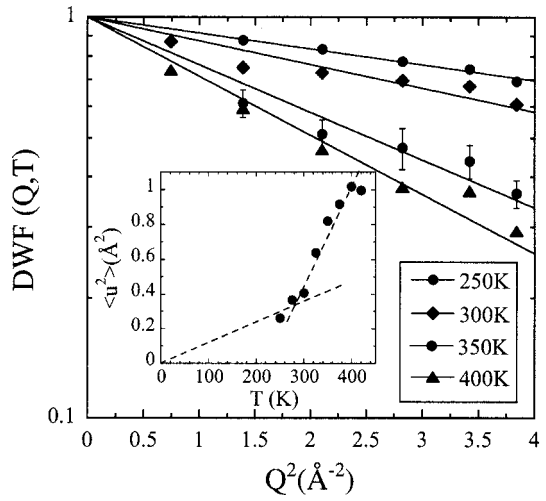

FIG. 7. Q dependence of the amplitude of the scattering functions (Debye–Waller factor) for the temperatures indicated. The error bars at 350 K show the uncertainties associated to the assumptions about the coherent contribution (see the text). Lines through the points are fits to Eq. (8). The insert shows the obtained values for the mean-squared displacement as a function of temperature. The dotted lines are guides for the eye.

with the VF law describing the dipolar data, within the uncertainties. The time scale obtained for 375 K (the lowest temperature at which we can fit this component) could show, however, a tendency to deviate towards a weaker dependence.

At this point, we may comment that, in the case of PES, the local dynamics is very rich, as shown by QENS measurements in the glassy state.[47] Its phenylene rings undergo oscillations and π-flips which are thought to be the main responsible for the γ-relaxation. The characteristic time scales of both processes are accessible by the IN10 window in the high-temperature range investigated. In principle, the amplitude of the fast oscillations is not very significant and the largest-amplitude motions (π-flips) of phenylene rings should not give rise to quasielastic coherent signal—initial and final configurations are identical. Therefore, we have not considered them in our data analysis procedure. However, we cannot discard that there could be some influence of these motions in the dPES coherent signal at high temperatures. If these local processes were coupled to the structural relaxation, the complex resulting process could indeed give rise to a quasielastic contribution different from that corresponding to the isolated α-relaxation (of course, impossible to model without the help of, e.g., molecular dynamics simulations). This could explain the large difference between the dielectric spectroscopy and the QENS time scales. It could also be the responsible for the possible deviation at 375 K towards faster time scales as expected from the DS extrapolation. Unfortunately, the uncertainties involved in the data analysis do not allow us determining the extrapolation to low temperatures of the time scale of the coherent signal. Therefore, in the evaluation of the spectra at lower temperatures, we have considered two limiting scenarios for the timescale of the coherent contribution: (i) to follow the temperature dependence deduced from the DS results (i.e., the dashed line through the QENS data in Fig. 6, which leads to an elastic contribution for the coherent part at 350 K and below) and

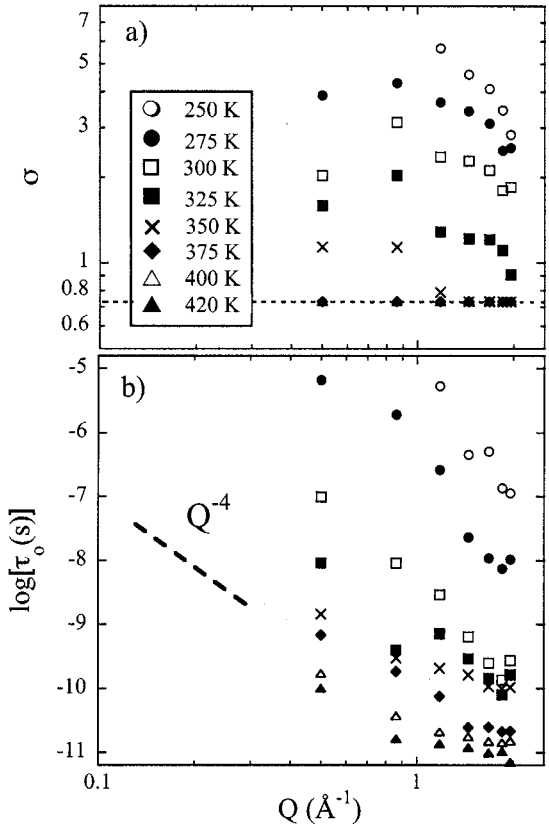

FIG. 8. Q dependence of the width (a) and the time of the maximum (b) of the log-normal distribution functions describing the PEO dynamics in the blend at several temperatures: 250 K (empty circles), 275 K (full circles), 300 K (empty squares), 325 K (full squares), 350 K (crosses), 375 K (diamonds), 400 K (empty triangles), and 420 K (full triangles). The dotted line in (a) shows the value σ=0.73 (closest distribution to that for a KWW function with β=0.5).

(ii) to follow an Arrhenius-type extrapolation of the QENS data. The only temperature for which the second case leads to a quasielastic broadening is 350 K. The ends of the vertical dashed-dotted line in Fig. 6 show the two extreme values considered for this temperature. For the lower temperatures investigated, both approximations are elastic.

For several temperatures, Fig. 7 shows the Q dependence of the amplitudes obtained from this fitting procedure. In the case of 350 K, the error bars cover the two extreme scenarios considered (elastic and quasielastic coherent contribution). These amplitudes follow well a DWF-type dependence [Eq. (8)], revealing the mean-squared displacement, $\langle u^2 \rangle$, associated to the fast dynamical processes in the system (shown in the insert). The values obtained for $\langle u^2 \rangle$ are of the same order as those obtained, e.g., in the cases of the homopolymers head-to-head polypropylene and poly(ethylene propylene) and their blend.[13] We note that the sharp increase of this function above the low-temperature (glassy) estimation starts already at temperatures below the average glass-transition of the blend, i.e., closer to the glass-transition temperature of pure PEO.

Turning to the dynamics of PEO hydrogens in the blend, the analysis of the QENS spectra allowed determining the width σ and position of the maximum τ_o of the distribution of relaxation times $g(\log \tau)$ in the framework of our model.

The results obtained are shown in Fig. 8. Let us first focus on the high-T regime investigated between 375 and 420 K. There, the values of σ were found to be close or even slightly below 0.73. This is the value of the width of the distribution $g(\log \tau)$ closest to the distribution $g_w^{\beta=0.5}(\log \tau)$ corresponding to a KWW relaxation function with $\beta=0.5$. We note that this is the expected spectral shape in the case of a polymer in equilibrium well above the glass transition, free of any confinement effect—in fact, PEO homopolymer shows such spectral shape in the high-temperature range.[18] Therefore, in this temperature region, we can assume that the PEO component behaves as a "standard" glass-forming polymer and have fixed the value of σ to 0.73. The Q dependence of the such obtained characteristic times is compatible with the behavior expected in such a situation: an assymptotic Gaussian Q dependence $\tau \propto Q^{-2/\beta}$ in the low-Q region and deviations to a weaker dependence above ≈ 1 Å^{-1} (see, e.g., Refs. 48 and 49). At lower temperatures, the width of $g(\log \tau)$ dramatically increases with decreasing temperature. The σ values shown for 350 K in Fig. 8 correspond to the case when the coherent contribution is considered as elastic. For simplicity, we have not included the values obtained assuming the other approximation, which are of the order of 15% higher. It is worth noting that, at 250 K, σ takes values from 3 to 6 decades. Within the uncertainties, this parameter seems to have some tendency to increase toward lower Q values (equivalently, larger length scales). A similar tendency has been reported for PEO in blends with PVAc.[21] Simultaneously, within the uncertainties, the Q dependence of the characteristic time seems to remain close to Q^{-4}. Taking into account the large deviations of the spectral shape with respect to a KWW with $\beta=0.5$, such dispersions imply severe deviations from Gaussian behavior.[50] These features—large broadening, non-Gaussian behavior—can be interpreted as signatures of heterogeneous and localized (confinedlike) motions detected by IN10.

Nowadays, it is well known that in a polymer blend in equilibrium the segmental α-relaxation time of one of the components is usually well described by the same VF expression [Eq. (11)] of the corresponding homopolymer but with a different value of T_o (or T_g). This new (effective) T_o (T_g) value can be calculated, for instance, in the framework of the Lodge and McLeish model[1] based on the self-concentration ideas. This was the procedure followed by us in our previous works to estimate the expected behavior of PEO in PEO/PMMA and PEO/PVAc blends.[21] Here, we have followed the same procedure, in which we assume a value of 0.15 for the self-concentration of PEO. Figure 6 shows both the VF law for pure PEO and that corresponding to PEO in PEO/PES blend. As can be seen, the data obtained for PEO in the blend are compatible with this curve only at high temperatures. We note that the temperature dependence of the PEO characteristic time scales is much weaker and, below $\approx$325 K, it strongly deviates from the behavior expected for its segmental relaxation. Note that, in principle, in this range the coherent signal is elastic even if we consider possible local contributions. In fact, it is also noteworthy that the value of the timescale obtained for PEO in the blend at 350 K is rather insensitive to the approach considered for the coherent contribution: the error bar obtained is of the order of the point size shown in Fig. 6. In the low-temperature range investigated, the PEO time scale seems to approach, within the experimental uncertainties, the extrapolation of the timescales obtained for the so-called secondary γ-process in semicrystalline PEO (percentage of crystallinity of the order of 70–80) as obtained by dielectric spectroscopy.[51] This can be realized from Fig. 6, where the QENS results at $Q=1.45$ Å^{-1} are displayed together with the dielectric data reported in Ref. 51. We also note that, as in the case of our neutron scattering results, the γ-relaxation function measured by dielectric spectroscopy is a rather broad and symmetric process. However, whether or not the microscopic motions of PEO in the blend here investigated correspond to those involved in the γ-relaxation of PEO is a question that deserves further work and which is beyond the scope of this paper.

Before going on with the discussion on the results, we comment on the reliability of the values obtained in our data analysis procedure, in particular, of those corresponding to the low-temperature region. The approach followed involves two contributions (coherent and incoherent) and the choice of a functional form for the PEO hydrogens scattering function (log-normal distribution). At low temperatures, we have justified the elastic assumption of the coherent contribution, which is fixed. Then, we allow only three parameters to float: the DWF, the width, and the time scale of the distribution. Of course, these parameters are coupled. However, we can impose a consistency in the obtained values. In this sense, obtaining a reasonable Q dependence of the amplitude (with a sensible $\langle u^2 \rangle$ value) can be taken as a criterion to set bounds for the shape of the function. Then, it turns out that the σ values have to increase when Q decreases (Fig. 8). Once the shape of the function is determined within some uncertainty, the estimated error for the time scale is not so large—note that the broadening of the spectra at low temperature is significant in the intermediate-Q range [Figs. 3(a) and 4]. For example, for the points shown in Fig. 6 the errors amount to ± 0.3 decades for 275 K and ± 0.7 decades for 250 K. Concerning the choice of the log-normal distribution function, we have considered the, in principle, simplest functional form one can assume. We are aware that the function could be much more complex; in fact, molecular dynamics simulations point to very stretched functional forms with some crossover from a convex to concave behavior with increasing Q.[10,18] Unfortunately, the limited dynamic window of backscattering instruments prevents a more sophisticated approach for the functional form of the PEO correlation function. However, our analysis clearly show—beyond all the possible involved uncertainties—that there is a *qualitative* difference between the dynamical features of PEO at low and high temperatures.

Thus, as in the case of the blends with PMMA (Ref. 18)—and more evidently with PVAc (Refs. 21 and 24)—we seem to witness a crossover in the dynamics of PEO from "standard" glass-forming polymerlike at high temperatures to a different regime characterized by extremely broad distributions of relaxation times and strong deviations from Gaussian behavior and from the typical VF-temperature de-

pendence when freezing. As above mentioned and proposed in previous works,[18,21] we interpret this behavior as a consequence of the freezing of the segmental motions of the surrounding slow and majority component (dPES in this case). The concept of dynamical asymmetry (ratio between the characteristic time scales of the components in a multicomponent system) plays the essential role in this scenario. In miscible polymer blends, the dynamical asymmetry is induced by the intrinsic dynamic heterogeneity due to self-concentration effects. Well above $\langle T_g^{\text{blend}} \rangle$ the dynamic asymmetry is not very large: we can see from Fig. 6 that the relaxation time observed for dPES is less than two orders of magnitude slower than the incoherent time scale of PEO hydrogens. However, as the temperature decreases towards $\langle T_g^{\text{blend}} \rangle$ (which is mainly determined by the majority component dPES), the structural relaxation of the slow component rapidly freezes and the dynamic asymmetry increases (note that this should happen independently of any additional local contribution as the π-flips of the rings). As can be seen in Fig. 6, in the temperature region of the glass transition of the blend, the difference between the time scale of the structural relaxation of dPES and PEO in the blend (dynamic asymmetry) increases up to more than six orders of magnitude. Therefore, in this temperature range the rearrangements of the surrounding environment of PEO are so slow compared to its own segmental motions, that this component is somehow confined within a rigid matrix. Consequently, PEO motions become localized and heterogeneous and show the features of confined motions.

Do these observations depend on the nature of the other blend component? Figure 6 compares the results obtained in the three blends investigated by QENS until now. The PEO motions in PEO/PMMA (Ref. 18) and PEO/PVAc (Refs. 21 and 24) (which time scales are represented by squares and circles, respectively) were also found to deviate from the Lodge and McLeish prediction under high dynamic asymmetry conditions. PEO seems to behave in a very similar way surrounded by slow or frozen PMMA and PVAc. However, obviously its motions are slower in a rigid PES environment and might be related in some way to the γ-relaxation process of semicrystalline PEO. It is worthy of remark that the γ-relaxation of PEO is also observed (unchanged) by dielectric spectroscopy in blends of amorphous PEO with other components.[21,52] Therefore, it has been assigned to motions of noncrystalline segments of PEO. Thus, we suggest that in the case of this blend, the local motions performed by PEO in the rigid PES surrounding are very similar to those taking place in the amorphous regions of pure PEO below its glass transition. Apparently, PES provides an environment for PEO which seems to be effectively very similar to its own, and therefore the confined motion shows the features of the secondary process in the pure polymer. We emphasize that this is not the regular case, as demonstrated for PEO in PEO/PMMA,[18] and PEO/PVAc.[21]

We may seek the reason for this qualitative difference in the intermolecular packing in the different samples. As we have previously discussed, the first structure factor peak presumably revealing interchain correlations is roughly at the same position in both polymers, PES and PEO [see Figs. 2(b) and 9]. This would suggest very similar intermolecular distances and packing. On the contrary, as can be seen in Fig. 9, the structure factors of PMMA and PVAc display pronounced peaks at significantly smaller Q values, corresponding to much larger interchain distances[53,54] and consequently showing looser packing than pure PEO. For this reason, the free volume available for PEO segments in PMMA and PVAc matrices is probably bigger than in PES surrounding and even in pure PEO environment. This would allow the occurrence of fast motions for PEO—note that they could be even faster than in the homopolymer. We would like to mention that, apparently, this is the case of the blends of PVME/PS, where PVME confined motions faster than in pure PVME have also been reported.[12,55]

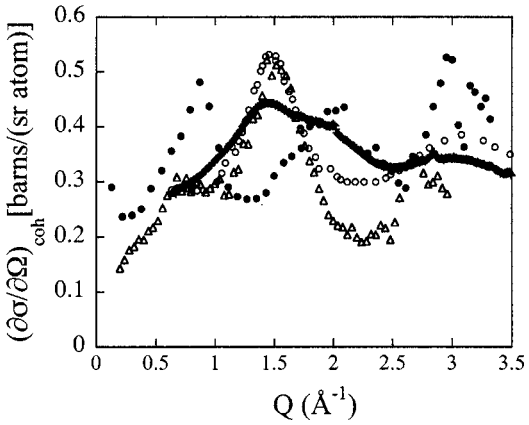

FIG. 9. Comparison of the static structure factors for the polymers considered: PMMA at 300 K (full circles) (Ref. 18), PVAc at 400 K (triangles) (Ref. 21), PES at 300 K (crosses), and PEO (empty circles) (Ref. 26).

In addition, the existence of polar interactions between the two blend components in the blend PEO/PES could be another reason for such a difference, with the PEO segments that are slowed down due to their interaction with the slow PES matrix. Note that such interactions are not reported for PEO/PMMA and PEO/PVAc blends. We could also suggest a possible coupling to some local motion in the blend (given the richness of PES local processes) as the reason for this different behavior in PES/PEO mixtures.

V. CONCLUSIONS

QENS with isotopic labeling has allowed us to selectively study the PEO hydrogen dynamics in the diluted blend PES/PEO. In the neighborhood of $\langle T_g^{\text{blend}} \rangle$, the behavior of the fast (PEO) component hints to a crossover from standard polymer meltlike dynamics at high temperatures towards a glassylike dynamics characterized by an Arrhenius temperature dependence and extremely broad distributions of relaxation times. In fact, the observed features of the PEO motions in this region, where these segments move within the rigid PES network, are very similar to those of the secondary γ-relaxation in neat semicrystalline PEO. Thus, the confinement effects in this blend show clear differences with respect to those found for PEO in blends with PVAc and PMMA. In those cases, the local PEO motions were clearly faster than the γ process. The origin of this observation might be sought in an excess of free volume offered by PVAc and PMMA

matrices to PEO segments with respect to that available in the neat system. Apparently, the stronger interactions with PES and mightbe the more closely packed surround lead to a localized dynamics of PEO in the blend with PES which is rather similar to that observed in the amorphous regions of pure semicristalline PEO.

ACKNOWLEDGMENTS

We thank Angel Alegría and Jürgen Allgaier for fruitful discussions and Thomas Hansen and Iban Quintana for their help at D20. This research project has been supported by the European Commission NoE SoftComp, Contract No. NMP3-CT-2004-502235, the "Donostia International Physics Center." A.A. and J.C. acknowledge support from the projects MAT2007-63681, IT-436-07 (GV), and the Spanish Ministerio de Educacion y Ciencia (Grant No. CSD2006-53).

[1] T. P. Lodge and T. C. B. McLeish, Macromolecules **33**, 5278 (2000).
[2] E. Leroy, A. Alegría, and J. Colmenero, Macromolecules **36**, 7280 (2003).
[3] Y. Hirose, O. Urakawa, and K. Adachi, Macromolecules **36**, 3699 (2003).
[4] Y. He, T. R. Lutz, and M. D. Ediger, J. Chem. Phys. **119**, 9956 (2003).
[5] R. Kant, S. K. Kumar, and R. H. Colby, Macromolecules **36**, 10087 (2003).
[6] R. H. Colby and J. E. G. Lipson, Macromolecules **38**, 4919 (2005).
[7] E. Krygier, G. Lin, J. Mendes, G. Mukandela, D. Azar, A. A. Jones, J. A. Pathak, R. H. Colby, S. K. Kumar, G. Floudas, R. Krishnamoorti, and R. Faust, Macromolecules **38**, 7721 (2005).
[8] Y. Hirose and K. Adachi, Macromolecules **39**, 1779 (2006).
[9] C. M. Roland, K. J. McGrath, and R. Casalini, Macromolecules **39**, 3581 (2006).
[10] J. Colmenero and A. Arbe, Soft Matter **3**, 1474 (2007).
[11] G.-C. Chung, J. A. Kornfield, and S. D. Smith, Macromolecules **27**, 5729 (1994).
[12] C. Lorthioir, A. Alegría, and J. Colmenero, Phys. Rev. E **68**, 031805 (2003).
[13] R. Pérez Aparicio, A. Arbe, J. Colmenero, W. Schweika, W. Richter, and L. J. Fetters, Macromolecules **39**, 1060 (2006).
[14] I. Cendoya, A. Alegría, J. M. Alberdi, J. Colmenero, H. Grimm, D. Richter, and B. Frick, Macromolecules **32**, 4065 (1999).
[15] A. Arbe, A. Alegría, J. Colmenero, S. Hoffmann, L. Willner, and D. Richter, Macromolecules **32**, 7572 (1999).
[16] S. Hoffmann, L. Willner, D. Richter, A. Arbe, J. Colmenero, and B. Farago, Phys. Rev. Lett. **85**, 772 (2000).
[17] M. Doxastakis, M. Kitsiou, G. Fytas, D. N. Theodorou, N. Hadjichristidis, G. Meier, and B. Frick, J. Chem. Phys. **112**, 8687 (2000).
[18] A.-C. Genix, A. Arbe, F. Alvarez, J. Colmenero, L. Willner, and D. Richter, Phys. Rev. E **72**, 031808 (2005).
[19] V. García Sakai, J. K. Maranas, Z. Chowdhuri, I. Peral, and J. R. D. Copley, J. Polym. Sci., Part B: Polym. Phys. **43**, 2914 (2005).
[20] B. Farago, C. Chen, J. K. Maranas, S. Kamath, R. H. Colby, A. J. Pasquale, and T. E. Long, Phys. Rev. E **72**, 031809 (2005).
[21] M. Tyagi, A. Arbe, J. Colmenero, B. Frick, and J. R. Stewart, Macromolecules **39**, 3007 (2006).
[22] V. García Sakai, C. Chen, J. K. Maranas, and Z. Chowdhuri, Macromolecules **37**, 9975 (2004).
[23] J. Liu, V. García Sakai, and J. K. Maranas, Macromolecules **39**, 2866 (2006).
[24] M. Tyagi, A. Arbe, A. Alegría, J. Colmenero, and B. Frick, Macromolecules **40**, 4568 (2007).
[25] K. Niedzwiedz, A. Wischnewski, M. Monkenbusch, D. Richter, A.-C. Genix, A. Arbe, J. Colmenero, M. Strauch, and E. Straube, Phys. Rev. Lett. **98**, 168301 (2007).
[26] J. A. Johnson, M.-L. Saboungi, D. L. Price, S. Ansell, T. P. Russell, J.-W. Halley, and B. Nielsen, J. Chem. Phys. **109**, 7005 (1998).
[27] W. Guo and J. S. Higgins, Polymer **32**, 12 (1991).
[28] T. Springer, *Quasielastic Neutron Scattering for the Investigation of Diffusive Motions in Solids, Liquids*, Springer Tracts in Modern Physics (Springer-Verlag, Berlin, 1972), Vol. 64.
[29] S. W. Lovesey, *Theory of Neutron Scattering from Condensed Matter* (Clarendon, Oxford, 1984).
[30] M. Bée, *Quasielastic Neutron Scattering* (Hilger, Bristol, 1988).
[31] G. L. Squires, *Introduction to the Theory of Thermal Neutron Scattering* (Dover, New York, 1996).
[32] Apart from inelasticity effects leading to a slight monotonous decay, the incoherent intensity does not depend on momentum transfer. On the other hand, limited integration over a certain bandpass on D7 (about 3 meV) might lead to underestimation of incoherent scattering at high temperatures, where the Debye–Waller factor might play an important role.
[33] J. S. Higgins and H. C. Benoit, *Polymers and Neutron Scattering* (Oxford University Press, Oxford, 1994).
[34] G. D. Wignall and Y. B. Melnichenko, Rep. Prog. Phys. **68**, 1761 (2005).
[35] B. Frick, D. Richter, and Cl. Ritter, Europhys. Lett. **9**, 557 (1989).
[36] D. Richter, M. Monkenbusch, A. Arbe, and J. Colmenero, *Neutron Spin Echo Investigations on Polymer Dynamics*, Advances in Polymer Science Vol. 174 (Springer Verlag, Berlin, 2005).
[37] Proceedings of the 3rd International Workshop on Dynamics in Confinement, edited by M. Koza, B. Frick, and R. Zorn [Eur. Phys. J. Spec. Top. 141 (2007)].
[38] N. G. McCrum, B. E. Read, and G. Williams, *Anelastic and Dielectric Effects in Polymeric Solids* (Dover, New York, 1967).
[39] *Broadband Dielectric Spectroscopy*, edited by F. Kremer and A. Schönhals (Springer Verlag, Heidelberg, 2002).
[40] J. Colmenero, A. Moreno, and A. Alegría, Prog. Polym. Sci. **30**, 1147 (2005).
[41] R. Zorn, A. Arbe, J. Colmenero, B. Frick, D. Richter, and U. Buchenau, Phys. Rev. E **52**, 781 (1995).
[42] In the case of incoherent scattering, it is more precise the term "Lamb–Mössbauer" factor; for simplicity, we call both prefactors "Debye–Waller."
[43] The parameters of the VF equation used for describing the DS data of the α-relaxation of dPES in the blend are $B=4598$, $\tau_o=1.5e-16$ s, and $T_o=203$ K.
[44] A. Arbe, D. Richter, J. Colmenero, and B. Farago, Phys. Rev. E **54**, 3853 (1996).
[45] J. Colmenero, F. Alvarez, and A. Arbe, Phys. Rev. E **65**, 041804 (2002).
[46] W. Götze, in *Liquids, Freezing, Glass Transition*, edited by J. P. Hansen, D. Levesque, and J. Zinn-Justin (North-Holland, Amsterdam, 1991), p. 287.
[47] I. Quintana, A. Arbe, J. Colmenero, and B. Frick, Macromolecules **38**, 3999 (2005).
[48] A. Arbe, J. Colmenero, F. Alvarez, M. Monkenbusch, D. Richter, B. Farago, and B. Frick, Phys. Rev. Lett. **89**, 245701 (2002).
[49] A. Arbe, J. Colmenero, F. Alvarez, M. Monkenbusch, D. Richter, B. Farago, and B. Frick, Phys. Rev. E **67**, 051802 (2003).
[50] The Gaussian approximation implies a $Q^{-2/\beta}$ dependence of the characteristic time (i.e., for $\beta=0.5$, $\tau \propto Q^{-4}$). Thus, for β values smaller than 0.5, this corresponds to Q dependences stronger than $\tau \propto Q^{-4}$. [J. Colmenero, A. Alegría, A. Arbe, and B. Frick, Phys. Rev. Lett. **69**, 478 (1992)].
[51] X. Jin, S. Zhang, and J. Runt, Polymer **43**, 6247 (2002).
[52] X. Jin, S. Zhang, and J. Runt, Macromolecules **37**, 8110 (2004).
[53] A.-C. Genix, A. Arbe, F. Alvarez, J. Colmenero, W. Schweika, and D. Richter, Macromolecules **39**, 3947 (2006).
[54] M. Tyagi, A. Arbe, F. Alvarez, J. Colmenero, and M. A. Gonzalez (unpublished).
[55] S. Koizumi, J. Polym. Sci., Part B: Polym. Phys. **42**, 3148 (2003).